



UNIVERSITÀ DI PARMA

DEPARTMENT OF ENGINEERING AND
ARCHITECTURE
MASTER'S DEGREE IN COMMUNICATION ENGINEERING

QUANTUM SEARCH FOR REALISTIC QUANTUM WALKS

Supervisor:

Prof. SANDRO MARCEL WIMBERGER

Thesis of:

MICHELE DELVECCHIO

ACADEMIC YEAR

2018-2019

To my family

"If you think you understand quantum mechanics, you don't understand quantum mechanics."

Richard Feynman

Contents

1	Introduction to Quantum Walks	3
1.1	Principles of quantum mechanics	3
1.1.1	Unitary evolution	4
1.1.2	Composite System	4
1.1.3	Measurement Process	5
1.1.4	Computational Basis	6
1.2	Quantum Walks	7
2	Continuous quantum walk	9
2.1	Quantum kicked rotor	9
2.1.1	Quantum resonances	10
2.2	Continuous-Time Quantum Walk	12
3	Superposition of Eigenstates as Initial State	19
3.1	Superposition in δ -Kicked Rotor (QKR)	19
3.1.1	Numerical Simulations	21
3.2	Superposition in Continuous-Time Quantum Walk (CTQW)	23
3.3	Extension to general initial state	28
4	Quantum Search	31
4.1	Searching Problem	31
4.2	Search algorithm using QKR	33

4.2.1	Performance	39
5	Conclusions and future developments	43
5.1	Conclusions	43
5.2	Future developments	45
A	Bessel identity check	47
A.1	Modified Vandermonde's identity	48

Introduction

Technology is a big part of the world economy. Companies continuously try to win new challenges in order to introduce very often competitive and innovative products on the market. One of most challenging innovation is the Quantum Computer or more in general the Quantum Technologies. According to many scientists, quantum technology can provide a computational power much higher than the classical counterpart. For this reason the biggest companies such as Google [1], IBM, Rigetti and D-Wave [2] are investing enormous amount of money to be the first to achieve this breakthrough. Due to the difficulty of realizing a quantum computer and the variety of disciplines involved, the problem is not only of interest in technological fields, but also in Physics. In fact there are still many challenges to be overcome in the fundamental fields of physics in order to build a quantum computer.

Although there are many limitations and many problems to be solved, theoretical scientists are working on more and more efficient quantum algorithms and one approach in this direction exploits *Quantum Walk*. It is not simple to realize experimentally a quantum walk and in the literature there are not so many experiments. On the subject so far, the Quantum Walk, in particular the continuous time version (CTQW) which is the one studied in this thesis, has been realized, for instance, with optical cavities [3], nuclear spins in magnetic field [4], polarization of single photons [5] and recently with (ultra)cold-atoms [6].

In this thesis work we give a mathematical proof of the analogy between the Quantum Kicked Rotor (QKR), which is a standard model used in the Quantum Chaos field,

at quantum resonance and the CTQW according to the formulation of the Portugal's book. This study can lead to several applications since we can implement algorithms based on quantum walks in an experimental working system. Among the possible applications we propose a search protocol for the experimental CTWQ obtained using the (ultra)cold-atoms technique. The thesis is organized as follows: in the first chapter we will see a very short introduction about the postulates of quantum mechanics that we need for our purpose; the second chapter, after some theory about the QKR, shows the first result of the work which is the relation between the evolution of QKR in resonance conditions and the CTQW; then a generalization with an initial state given by a superposition of more eigenstates is explained in the third chapter; the last chapter, instead, shows a possible application of the QKR to perform a quantum search algorithm. The majority of this work, has been summarized in the paper [7].

Chapter 1

Introduction to Quantum Walks

The classical random walk is a well known problem and it is described by vectors and matrices. In analogy with the classical case, the quantum walk is described by vectors and operators in Hilbert space. For this reason in the first part of this chapter we will see the postulates of quantum mechanics used to work with quantum walks and in the second one we will briefly explain the difference between the classical and the quantum walk. For the first section I followed the Portugal's book [8] which is a good introduction also to the quantum walks.

1.1 Principles of quantum mechanics

The state of a physical system describes its physical characteristics at a given time. A general state $|\psi\rangle$ is represented by a vector in the Hilbert space, which is complex. Because of the completeness of the Hilbert space, every state $|\psi\rangle$ can be written as linear combination of basis vectors. So the power of quantum mechanics is that one state can be in a superposition of basis states. This feature is of fundamental relevance for quantum walks and for our results in chapter 3.

Let us take the spin of an electron, as example, which can assume only two values: "*spin up*", "*spin down*". In this Hilbert space \mathbb{C}^2 , we describe the "*spin up*" using the

vector

$$|0\rangle = \begin{bmatrix} 1 \\ 0 \end{bmatrix},$$

and "spin down"

$$|1\rangle = \begin{bmatrix} 0 \\ 1 \end{bmatrix}.$$

The spin state of the electron is described by a linear combination of vector $|0\rangle$ and $|1\rangle$

$$|\psi\rangle = a_0 |0\rangle + a_1 |1\rangle. \quad (1.1)$$

The coefficients a_0 and a_1 are complex and they satisfy the following relation

$$|a_0|^2 + |a_1|^2 = 1. \quad (1.2)$$

Since $|0\rangle$ and $|1\rangle$ are orthogonal, the sum cannot be zero. From this notation, we interpret the quantities $|a_0|^2$ and $|a_1|^2$ as the probability of being in the *spin up* or *spin down*.

1.1.1 Unitary evolution

As many things in nature, the state of a quantum system evolves in time as well. This evolution is described by an unitary operator U . For instance if we have the state $|\psi(0)\rangle$ at time t_0 , the state $|\psi(t)\rangle$ at time t is obtained by applying the operator U to the state $|\psi(0)\rangle$

$$|\psi(t)\rangle = U |\psi(0)\rangle. \quad (1.3)$$

In general, given a physical context, the operator U is found by solving the famous Schrödinger's equation.

1.1.2 Composite System

According to the postulate of the composite system, the state space of a composite system is the tensor product of the state space of the components. If $|\psi_1\rangle, |\psi_2\rangle, \dots, |\psi_n\rangle$ describe the state on n isolated quantum systems, the state of the composite system is $|\psi_1\rangle \otimes |\psi_2\rangle \otimes \dots \otimes |\psi_n\rangle$.

An example of such a type of systems is the memory of a n -qubit quantum computer. Usually, the memory is divided into sets of qubits called *registers*. Every qubit live in an Hilbert space of dimension 2, \mathbb{C}^2 . So the state space of one register is the tensor product of each qubit. Then the state space of the entire memory is the tensor product of the Hilbert space of each register.

1.1.3 Measurement Process

In a classical world, namely the non-quantum world, the measurement process is a process of knowing classical information about a system. It can be performed using devices such as rules, scales or chronometers. However for a quantum system things are not so straightforward. In fact measuring a quantum system that is in unknown state means perturbing or disturbing the state irreversibly. After performing the measurement on a quantum system, you cannot know in which state the system was before the measurement.

In quantum mechanics, the *projective measurements*, which is a special class of measurement, are described by an *observable*, O , that is a Hermitian operator acting on the Hilbert space of the state space of the system. The observable O has a spectral decomposition

$$O = \sum_{\lambda} \lambda P_{\lambda}, \quad (1.4)$$

where P_{λ} is the projector onto the eigenspace of O associated with the eigenvalue λ . An important concept is that the possible outcomes of a measurements of the observable O , are the eigenvalues λ .

If the system state at the time of measurement is $|\psi\rangle$, the probability of obtaining the result λ is

$$p_{\lambda} = \langle \psi | P_{\lambda} | \psi \rangle, \quad (1.5)$$

or equivalently

$$p_{\lambda} = \|P_{\lambda} |\psi\rangle\|^2. \quad (1.6)$$

Therefore given the outcome λ , the normalized state of the quantum system immediately after the measure is

$$\frac{P_\lambda |\psi\rangle}{\sqrt{p_\lambda}}. \quad (1.7)$$

1.1.4 Computational Basis

The computational basis is the basis that we use when we measure a quantum system with an observable. It belongs to the Hilbert space and in general, for a n qubits system, it is the set $\{|0\rangle, |1\rangle \dots |2^n - 1\rangle\}$ in the decimal notation. So we can write the observable as

$$O = \sum_{\lambda=0}^{2^n-1} \lambda P_\lambda, \quad (1.8)$$

where $P_\lambda = |\lambda\rangle \langle \lambda|$. From the theory of quantum mechanics we know that every state of a system can be written as a linear combination of eigenstates. Thus for a n qubits system, a generic state can be written as

$$|\psi\rangle = \sum_{\lambda=0}^{2^n-1} a_\lambda |\lambda\rangle. \quad (1.9)$$

If we evaluate the probability using the equation (1.5), we get

$$p_\lambda = \langle \psi | P_\lambda | \psi \rangle = |a_\lambda|^2. \quad (1.10)$$

This latter equation tells us that the probability of obtaining λ as the result of a measurement is given by $|a_\lambda|^2$. For this reason we have to be sure that the sum of probabilities is 1 and therefore the a_λ must satisfy the constraint

$$\sum_{\lambda} |a_\lambda|^2 = 1. \quad (1.11)$$

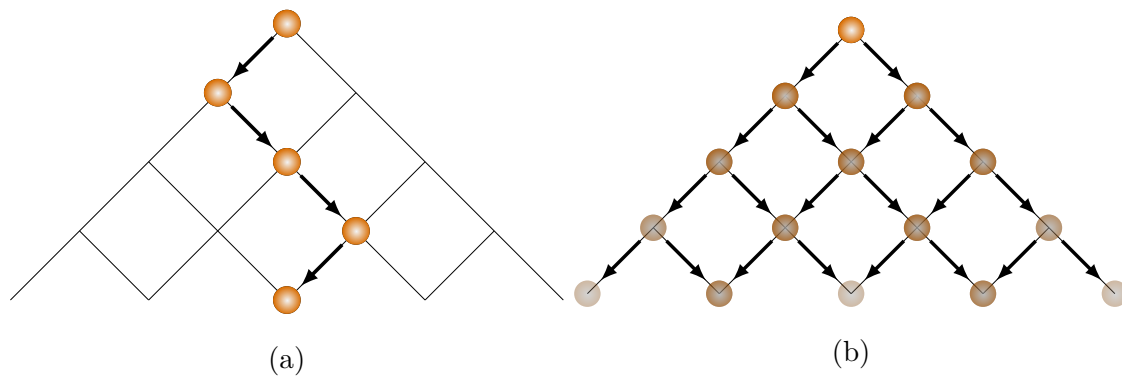


Figure 1.1: (a) Classical Random Walk of a classical particle; (b) Quantum Random Walk of a quantum particle.

1.2 Quantum Walks

Random walks are a well studied classical problem. Let us imagine a ball which is positioned at the centre of a line that we will call *position* 0. The ball can move either to the left or to the right, with the same probability, every time we toss a coin. After tossing the coin t times, the most likely position of the ball will be the starting point, namely 0. Figure 1.1a shows exactly this behaviour. In mathematical language, we say that the probability distribution of the position of the ball is a *Gaussian* distribution centred on the mean position which is 0 and with variance σ . The variance represents the width of the distribution but we will deal with it in the next chapters.

Quantum walks are different from classical ones. At each tossing coin (this time it is a quantum coin), the particle will be in a superposition of states, which means that you can find the particle either on the left or on the right with the same probability. This property derives directly from quantum mechanics. Figure 1.1b shows, for instance, that at the first step the particle is split in two halves, one on the left and one on the right. Repeating this procedure many times, leads to a probability distribution completely different from the classical case. In fact the distribution of a quantum walk generated by an initial state composed of only one state, presents two peaks almost at the edges. This means that in the quantum case it is more likely to find the particle

at the border of the line. Indeed the last step of the figure 1.1b shows that in two points the particle is more visible than the other three. The origin of the different form the probability distribution derives from the textitquantum interference of the various paths. This effect occurs only in the quantum case and not in the classical one.

There are two kinds of quantum walks: *discrete* and *continuous*. The difference between the two is that the discrete walk needs a coin, as just seen above, while the continuous walk does not. In this work we will concentrate only on the latter walk and more details will be given in the next chapter.

Chapter 2

Continuous Quantum Walk through Quantum Kicked Rotor

The quantum δ -Kicked Rotor (QKR) is a theoretical model used in quantum chaology and it is very important for studying quantum effects such as dynamical localization and quantum resonances [9]. In this work we will exploit the latter effect in order to connect the QKR to a Quantum Walk (QW).

2.1 Quantum kicked rotor

Although the QKR is a theoretical model, it has been realized experimentally using techniques of atom optics. Basically a cold atom is exposed to short pulses (kicks) of a standing wave [10]. Its dynamics is described by the Hamiltonian

$$\hat{\mathcal{H}}(t) = \frac{\hat{P}^2}{2} + k \cos(\hat{X}) \sum_{t'=-\infty}^{+\infty} \delta(t - \tau t') \quad (2.1)$$

where \hat{P} and \hat{X} are the momentum and position operator respectively, τ is the kick period in dimensionless units and k its strength [9]. The evolution between two consecutive kicks is described by the unitary Floquet operator:

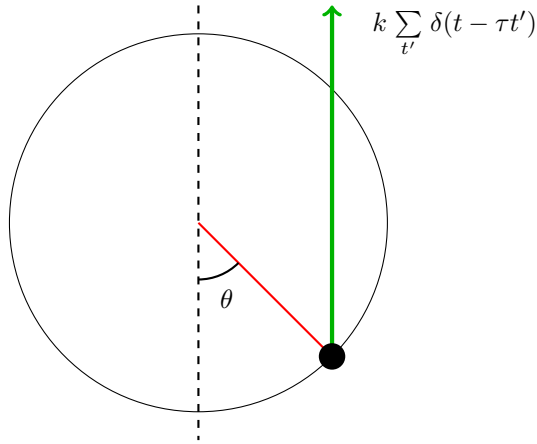


Figure 2.1: Classical approximation of a Quantum Kicked Rotor

$$\hat{U} = e^{-ik \cos(\hat{X})} e^{-i\tau \hat{P}^2/2} \quad (2.2)$$

However the theoretical treatment is simplified letting the QKR move on a circle instead of a line. Figure 2.1 shows a representation of this kicked rotor which can be approximated with a classical pendulum with pulsed gravity.

Since this system has a periodicity of the kicks, we can use a different representation of the unitary Floquet operator:

$$\hat{U}_\beta = e^{-ik \cos(\hat{\theta})} e^{-i(\tau/2)(\hat{N}+\beta)^2} \quad (2.3)$$

where β is the quasi-momentum (QM), namely the fractional part of the momentum p (from Bloch theory), $\hat{\theta}$ represents the space coordinate and \hat{N} is the angular momentum in the $\hat{\theta}$ representation: $\hat{N} = -id/d\theta$, now with periodic (circle) boundary conditions.

2.1.1 Quantum resonances

The time evolution determined by the operator (2.3) preserves many dynamical properties of the standard QKR (corresponding to $\beta = 0$), but not necessarily the quantum resonances. These occurs whenever $\tau = 4\pi p/q$, with p, q mutually integers, and $\beta = \frac{m}{2p}$

with m integer such that $0 \leq m \leq 2p$, because the operator (2.3) commutes with translations in momentum space by multiples of q [9].

We will concentrate only in the principal resonances $q = 1, 2$ so we set $\tau = 2\pi\ell$, with ℓ a positive integer. Substituting it in (2.3) and using the identity $\exp(-i\pi n^2\ell) = \exp(-i\pi n\ell)$, being n the eigenvalues of the angular momentum $\hat{\mathcal{N}}$, we obtain

$$\hat{\mathcal{U}}_\beta = e^{-ik \cos(\hat{\theta})} e^{-i\xi \hat{\mathcal{N}}} \quad (2.4)$$

where $\xi = \pi\ell(2\beta \pm 1) \bmod(2\pi)$ will be taken in $[-\pi, \pi)$.

If we choose as initial state the following plane wave of momentum $p_0 = n_0 + \beta_0$

$$\psi_\beta(\theta) = \frac{1}{\sqrt{2\pi}} \delta(\beta - \beta_0) e^{in_0\theta}, \quad (2.5)$$

in resonance regime $\xi = 0$ because it takes the constant value $\xi_0 = \pi\ell(2\beta_0 - 1)$ with $\beta_0 = \frac{1}{2} + \frac{n}{\ell} \bmod(1)$, $n = 0, 1, \dots, \ell - 1$, that are the resonant values of β . So the time evolution operator becomes

$$\hat{\mathcal{U}}_\beta = e^{-ik \cos(\hat{\theta})}. \quad (2.6)$$

We do not need β anymore, so let us neglect it to simplify the notation. If we apply the operator in the equation (2.6) t times (or a total time t in units of τ) which correspond to the number of the kicks, we arrive to

$$\hat{\mathcal{U}}^t = e^{-ikt \cos(\hat{\theta})}. \quad (2.7)$$

At this point, applying (2.7) to a generic initial state leads to

$$(\hat{\mathcal{U}}^t \psi_\beta)(\theta) = e^{-ikt \cos(\hat{\theta})} \psi_\beta(\theta) \quad (2.8)$$

and therefore the amplitude probability in momentum basis is given by

$$\langle n | \hat{\mathcal{U}}^t \psi_\beta \rangle = \int_0^{2\pi} \frac{d\theta}{\sqrt{2\pi}} e^{-in\theta - ikt \cos(\hat{\theta})} \psi_\beta(\theta). \quad (2.9)$$

Now, substituting (2.5) in (2.9) we get

$$\langle n | \hat{\mathcal{U}}^t \psi_\beta \rangle = \int_0^{2\pi} \frac{d\theta}{\sqrt{2\pi}} e^{-in\theta - ikt \cos(\hat{\theta})} \frac{1}{\sqrt{2\pi}} \delta(\beta - \beta_0) e^{in_0\theta}. \quad (2.10)$$

Since we are in resonance conditions, $\beta = \beta_0$, we can remove the subscript also from ψ .

With this notation we have

$$\begin{aligned} \langle n | \hat{\mathcal{U}}^t \psi \rangle &= \frac{1}{2\pi} \int_0^{2\pi} d\theta e^{-i(n-n_0)\theta - ikt \cos(\theta)} \\ &= -i^n J_{n-n_0}(kt), \end{aligned} \quad (2.11)$$

where in the last equality we have used the identity of Bessel function [9.1.21] from [11] which is

$$\frac{1}{2\pi} \int_{\alpha}^{\alpha+2\pi} d\theta e^{iz \cos(\theta)} e^{-in\theta} = i^n J_n(z). \quad (2.12)$$

Finally the probability distribution in the basis of the momentum states $\{n\}_{n \in \mathbb{Z}}$ is found by taking the modulus squared of (2.11), that is

$$P(n, t | n_0) = |J_{n-n_0}(kt)|^2. \quad (2.13)$$

Figure 2.2 shows an example distribution of the QKR after 30 kicks. The important observation that we can make from the figure is that the behaviour of the QKR with resonance conditions is equal to that one of a Continuous-Time Quantum Walk (CTQW) [see [8], sec. 3.4]. Such observation leads to the first result of this thesis which is treated in the next chapter.

2.2 Continuous-Time Quantum Walk

Following Portugal's book, ref [8], we know that for any Hamiltonian H , the evolution operator is defined as

$$U(t) = e^{-iHt}. \quad (2.14)$$

In general, if the initial condition is $|\psi(0)\rangle$, the state at time t is

$$|\psi(t)\rangle = U(t) |\psi(0)\rangle \quad (2.15)$$

with probability distribution

$$p_k = |\langle k | \psi(t) \rangle|^2 \quad (2.16)$$

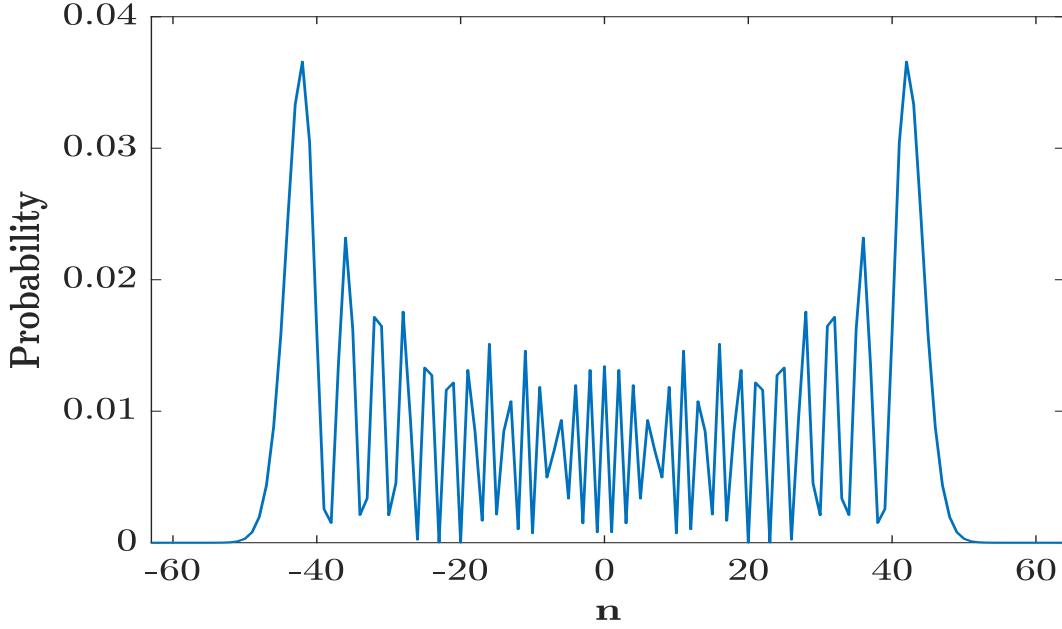


Figure 2.2: Example distribution in the space of the momentum state of the QKR after $t = 30$ kicks and with parameters $k = 1.5$, $n_0 = 0$.

where $|k\rangle$ is the state vector of the computational basis. If we consider the CTQW on a line, the Hamiltonian is

$$H_{ij} = \begin{cases} 2\gamma, & \text{if } i = j; \\ -\gamma, & \text{if } i \neq j \text{ and adjacent}; \\ 0, & \text{if } i \neq j \text{ and non-adjacent}; \end{cases} \quad (2.17)$$

therefore

$$H |n\rangle = -\gamma |n-1\rangle + 2\gamma |n\rangle - \gamma |n+1\rangle \quad (2.18)$$

Now we will prove that the probability distribution at a time t is $p(t, n) = |J_{|n|}(2\gamma t)|^2$. This problem is given as unsolved exercise in [8], No. 3.12.

Proof. First of all we will show by induction that matrix H of the CTQW on the line obeys

$$H^t |0\rangle = \gamma^t \sum_{n=-t}^t (-1)^n \binom{2t}{t-n} |n\rangle. \quad (2.19)$$

So let us start from $t = 1$

$$H|0\rangle = \gamma \sum_{n=-1}^1 (-1)^n \binom{2}{1-n} |n\rangle = -\gamma|-1\rangle + 2\gamma|0\rangle - \gamma|1\rangle .$$

Now assuming that it holds for a generic t , let us prove the relation for $t + 1$.

$$\begin{aligned} H^{t+1}|0\rangle &= HH^t|0\rangle = H \left(\gamma^t \sum_{n=-t}^t (-1)^n \binom{2t}{t-n} |n\rangle \right) = \\ &= -\gamma \left(\gamma^t \sum_{n=-t}^t (-1)^n \binom{2t}{t-n} |n-1\rangle \right) \\ &\quad + 2\gamma \left(\gamma^t \sum_{n=-t}^t (-1)^n \binom{2t}{t-n} |n\rangle \right) \\ &\quad - \gamma \left(\gamma^t \sum_{n=-t}^t (-1)^n \binom{2t}{t-n} |n+1\rangle \right) \end{aligned}$$

Now we change the variable $k = n - 1$ in the first term, $k = n$ in the second and $k = n + 1$ in the third. So we get:

$$\begin{aligned} &= -\gamma^{t+1} \sum_{k=-t-1}^{t-1} (-1)^{k-1} \binom{2t}{t-k-1} |k\rangle + 2\gamma^{t+1} \sum_{k=-t}^t (-1)^{k-1} \binom{2t}{t-k} |k\rangle \\ &\quad - \gamma^{t+1} \sum_{k=-t+1}^{t+1} (-1)^{k-1} \binom{2t}{t-k+1} |k\rangle \end{aligned}$$

The central term can be written as the sum of two equal quantities:

$$\begin{aligned} &= \gamma^{t+1} \left[- \sum_{k=-t-1}^{t-1} (-1)^{k-1} \binom{2t}{t-k-1} |k\rangle + \sum_{k=-t}^t (-1)^k \binom{2t}{t-k} |k\rangle \right. \\ &\quad \left. + \sum_{k=-t}^t (-1)^k \binom{2t}{t-k} |k\rangle - \sum_{k=-t+1}^{t+1} (-1)^{k+1} \binom{2t}{t-k+1} |k\rangle \right] \end{aligned}$$

We can change the sign of the first and the last term by taking out $(-1)^{\mp 1}$. Then we

can take some terms out of the summations:

$$\begin{aligned}
&= \gamma^{t+1} \left[\sum_{k=-t}^{t-1} (-1)^k \binom{2t}{t-k-1} |k\rangle + (-1)^k \binom{2t}{t-k-1} |k\rangle \Big|_{k=-t-1} \right. + \\
&\quad + \sum_{k=-t}^{t-1} (-1)^k \binom{2t}{t-k} |k\rangle + (-1)^k \binom{2t}{t-k} |k\rangle \Big|_{k=t} + \\
&\quad + \sum_{k=-t+1}^t (-1)^k \binom{2t}{t-k} |k\rangle + (-1)^k \binom{2t}{t-k} |k\rangle \Big|_{k=-t} + \\
&\quad \left. + \sum_{k=-t+1}^t (-1)^k \binom{2t}{t-k+1} |k\rangle + (-1)^k \binom{2t}{t-k+1} |k\rangle \Big|_{k=t+1} \right] =
\end{aligned}$$

Now we can add the first sum with the second one and the third sum with the fourth one, arriving to

$$\begin{aligned}
&= \gamma^{t+1} \left[\sum_{k=-t}^{t-1} (-1)^k \left[\binom{2t}{t-k-1} + \binom{2t}{t-k} \right] |k\rangle + (-1)^k \binom{2t}{t-k-1} |k\rangle \Big|_{k=-t-1} \right. + \\
&\quad + (-1)^k \binom{2t}{t-k} |k\rangle \Big|_{k=t} + \sum_{k=-t+1}^t (-1)^k \left[\binom{2t}{t-k} + \binom{2t}{t-k+1} \right] |k\rangle + \\
&\quad \left. + (-1)^k \binom{2t}{t-k} |k\rangle \Big|_{k=-t} + (-1)^k \binom{2t}{t-k+1} |k\rangle \Big|_{k=t+1} \right] =
\end{aligned}$$

We can use the following property of binomial coefficient:

$$\binom{n+1}{k+1} = \binom{n}{k+1} + \binom{n}{k}$$

so we get

$$\begin{aligned}
&= \gamma^{t+1} \left[\sum_{k=-t}^{t-1} (-1)^k \binom{2t+1}{t-k} |k\rangle + \sum_{k=-t+1}^t (-1)^k \binom{2t+1}{t-k+1} |k\rangle + \right. \\
&\quad + (-1)^k \binom{2t}{t-k-1} |k\rangle \Big|_{k=-t-1} + (-1)^k \binom{2t}{t-k} |k\rangle \Big|_{k=t} + \\
&\quad \left. + (-1)^k \binom{2t}{t-k} |k\rangle \Big|_{k=-t} + (-1)^k \binom{2t}{t-k+1} |k\rangle \Big|_{k=t+1} \right].
\end{aligned}$$

Thus we can take the terms with $k = t$ and $k = -t$ in the sums because their coefficient have the same structure, namely, it holds the following:

$$\binom{2t}{t-k} \Big|_{k=t} = \binom{2t}{0} = 1 = \binom{2t+1}{t-k} \Big|_{k=t} = \binom{2t+1}{0} \quad (2.20)$$

and also

$$\binom{2t}{t-k} \Big|_{k=-t} = \binom{2t}{2t} = 1 = \binom{2t+1}{t-k+1} \Big|_{k=-t} = \binom{2t+1}{2t+1} \quad (2.21)$$

So finally we have:

$$\begin{aligned} &= \gamma^{t+1} \left[\sum_{k=-t}^t (-1)^k \binom{2t+1}{t-k} |k\rangle + \sum_{k=-t}^t (-1)^k \binom{2t+1}{t-k+1} |k\rangle + \right. \\ &\quad \left. + (-1)^k \binom{2t}{t-k-1} |k\rangle \Big|_{k=-t-1} + (-1)^k \binom{2t}{t-k+1} |k\rangle \Big|_{k=t+1} \right] = \\ &= \gamma^{t+1} \left[\sum_{k=-t}^t (-1)^k \left[\binom{2t+1}{t-k} + \binom{2t+1}{t-k+1} \right] |k\rangle + \right. \\ &\quad \left. + (-1)^k \binom{2t}{t-k-1} |k\rangle \Big|_{k=-t-1} + (-1)^k \binom{2t}{t-k+1} |k\rangle \Big|_{k=t+1} \right] = \\ &= \gamma^{t+1} \left[\sum_{k=-t}^t (-1)^k \binom{2t+2}{t-k+1} |k\rangle + (-1)^k \binom{2t}{t-k-1} |k\rangle \Big|_{k=-t-1} + \right. \\ &\quad \left. + (-1)^k \binom{2t}{t-k+1} |k\rangle \Big|_{k=t+1} \right] = \\ &= \gamma^{t+1} \sum_{k=-t-1}^{t+1} (-1)^k \binom{2(t+1)}{t+1-k} |k\rangle = H^{t+1} |0\rangle \end{aligned}$$

where in the last equality we have included the extra terms into the sum, for the same reason explained in (2.20) and (2.21).

Now we have to compute $U(t) |0\rangle$. So let us start writing the operator as

$$U(t) |0\rangle = e^{-iHt} |0\rangle = \sum_{k=0}^{+\infty} \frac{(-iHt)^k}{k!} |0\rangle =$$

then we can apply the operator H using the previous result

$$= \sum_{k=0}^{+\infty} \frac{(-it)^k}{k!} \left(\gamma^k \sum_{n=-k}^k (-1)^n \binom{2k}{k-n} |n\rangle \right) =$$

at this point the two sums can be exchanged by changing the domain. This step is showed in figure 2.3 where the red area represents the original domain and the blue area is the new one. As we can see, the two areas are equal because the straight lines, $n = k$ and $n = -k$, split the rectangle in two equal parts. For this reason we can write

$$\begin{aligned}
&= \sum_{n=-\infty}^{+\infty} \sum_{k=|n|}^{+\infty} \frac{(-i\gamma t)^k}{k!} \overbrace{(-1)^{|n|}}^{e^{i\pi|n|}=e^{i(\frac{\pi}{2}+\frac{\pi}{2})|n|}} \binom{2k}{k-n} |n\rangle \\
&= \sum_{n=-\infty}^{+\infty} e^{i\frac{\pi}{2}|n|} e^{i\frac{\pi}{2}|n|} \sum_{k=|n|}^{+\infty} \frac{(-i\gamma t)^k}{k!} \binom{2k}{k-n} |n\rangle =
\end{aligned}$$

and using the identity for the Bessel function, to be demonstrated in appendix A,

$$e^{-2i\gamma t} J_{|n|}(2\gamma t) = e^{i\frac{\pi}{2}|n|} \sum_{k=|n|}^{\infty} \frac{(-i\gamma t)^k}{k!} \binom{2k}{k-n} \quad (2.22)$$

we get

$$= \sum_{n=-\infty}^{+\infty} e^{i\frac{\pi}{2}|n|-2i\gamma t} J_{|n|}(2\gamma t) |n\rangle = |\psi(t)\rangle$$

Now, as the last point, we can evaluate the probability distribution of a walker in the computational basis

$$\begin{aligned}
P(n, t) &= |\langle n| U(t) |\psi(0)\rangle|^2 = |\langle n|\psi(t)\rangle|^2 = \\
&= \left| \langle n| \sum_{k=-\infty}^{+\infty} e^{i\frac{\pi}{2}|k|-2i\gamma t} J_{|k|}(2\gamma t) |k\rangle \right|^2 = \\
&= \left| \sum_{k=-\infty}^{+\infty} e^{i\frac{\pi}{2}|k|-2i\gamma t} J_{|k|}(2\gamma t) \langle n|k\rangle \right|^2 = \\
&= \left| e^{i\frac{\pi}{2}|n|-2i\gamma t} J_{|n|}(2\gamma t) \right|^2 = |J_{|n|}(2\gamma t)|^2
\end{aligned} \quad (2.23)$$

□

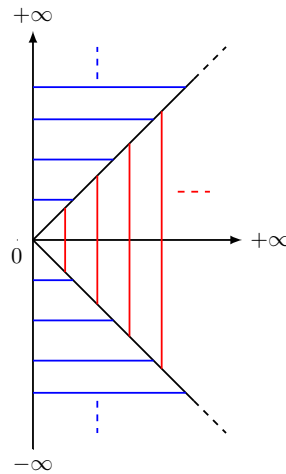


Figure 2.3: Domain of the sums. Horizontal lines represent the new area while the vertical one the original domain.

We have just proved that the walker's distribution of a Continuous-Time Quantum Walk [equation (2.23)] is equal to the one of the QKR at resonance [equation (2.13)]. Therefore we can use QKR in resonance conditions to implement a CTQW. As mentioned above, this is the first result of the thesis. In order to distinguish the equations of the QKR from those of the CTQW, let us add the γ subscript to the second case. So finally the new notation will be: H, P for the QKR and H_γ, P_γ for the CTQW.

Chapter 3

Superposition of Eigenstates as Initial State

Since we aim to implement a possible quantum search algorithm, as we will see in the chapter 4, we need a uniform distribution [8, 12]. So now we are going to extend the theory of single initial state, to the case where the initial state is given by a linear combination of three (and in one case, *five*) eigenstates.

3.1 Superposition in δ -Kicked Rotor (QKR)

While in section 2.2 we showed a probability distribution for an initial state composed of the eigenstate with eigenvalue $n_0 = 0$, that is

$$\psi(0) = \begin{pmatrix} \vdots \\ 0 \\ 1 \\ 0 \\ \vdots \end{pmatrix}, \quad (3.1)$$

in this section we will explore some cases with initial state given by a superposition of three eigenstates.

Let us consider a generic initial state whose population is described by coefficients vector C_n

$$\psi(0) = \mathcal{N} \begin{pmatrix} \vdots \\ C_{-2} \\ C_{-1} \\ C_0 \\ C_1 \\ C_2 \\ \vdots \end{pmatrix}, \quad (3.2)$$

where \mathcal{N} is the normalization constant and the C_n are complex coefficients of modulus 1 for simplicity. For our purpose, we take only $C_{-1}, C_0, C_1 \neq 0$ so the new initial state ψ is

$$\psi(\theta) = \frac{1}{\sqrt{3}} \frac{1}{\sqrt{2\pi}} (C_{-1}e^{-i\theta} + C_0 + C_1e^{i\theta}) \quad (3.3)$$

where we have the three components respectively with $n_0 = -1, n_0 = 0, n_0 = 1$. Now we can substitute it in the equation (3.5) getting

$$\langle n | \hat{\mathcal{U}}^t \psi \rangle = \frac{1}{\sqrt{3}} \int_0^{2\pi} \frac{d\theta}{2\pi} e^{-in\theta - ikt \cos(\hat{\theta})} (C_{-1}e^{-i\theta} + C_0 + C_1e^{i\theta}). \quad (3.4)$$

For more readable notation, equation (3.3) can be written as

$$\psi(\theta) = \frac{1}{\sqrt{3}} \frac{1}{\sqrt{2\pi}} (C_{-1} |-1\rangle + C_0 |0\rangle + C_1 |1\rangle). \quad (3.5)$$

Such notation will be also used in the next section of this chapter.

Solving the integral in the equation (3.4) in the same way we did in section 2.1.1, we obtain a sum of Bessel functions

$$\langle n | \hat{\mathcal{U}}^t \psi \rangle = \frac{1}{\sqrt{3}} [C_0 J_n(kt) + i(C_1 J_{n-1}(kt) - C_{-1} J_{n+1}(kt))]. \quad (3.6)$$

Therefore the distribution in the momentum space for general values of the C_n is

$$P(n, t) = \frac{1}{3} \{ |C_0|^2 J_n^2(kt) + |C_1|^2 J_{n-1}^2(kt) + |C_{-1}|^2 J_{n+1}^2(kt) + 2\Re[iC_0^* J_n(kt)(C_1 J_{n-1}(kt) - C_{-1} J_{n+1}(kt))] - 2\Re[C_{-1}^* C_1 J_{n-1}(kt) J_{n+1}(kt)] \}, \quad (3.7)$$

but in our case the coefficients have modulus equal to 1, so finally we arrive to

$$P(n, t) = \frac{1}{3} \{ J_n^2(kt) + J_{n-1}^2(kt) + J_{n+1}^2(kt) + 2\Re[iC_0^* J_n(kt)(C_1 J_{n-1}(kt) - C_{-1} J_{n+1}(kt))] + \\ - 2\Re[C_{-1}^* C_1 J_{n-1}(kt) J_{n+1}(kt)] \}. \quad (3.8)$$

This last equation is the general form of the Probability Density Function (PDF) for an initial state given by a superposition of *three* eigenstates. In the next section we will see how this probability distribution changes by choosing different values of C_n .

3.1.1 Numerical Simulations

Numerical simulation of QKR have been performed using Matlab. Mainly we simulated its evolution for 15 kicks, applying the operator (2.7), which means a Continuous-Time Quantum Walk (CTQW) of 15 steps. Then we evaluated the probability distribution and finally we applied the operator $(\hat{U}^t)^\dagger$ to perform the backward evolution. Figures 3.1, 3.2, 3.3 show some examples of probability distribution obtained with different choices of the coefficients C_n .

In particular for the first simulation we chose $C_1 = C_{-1} = C_0 = 1$ and $C_n = 0$ when $n \neq \pm 1, 0$. Figure 3.1a shows a lot of interference between neighbour momentum states, so we have lost the classical shape, with two peaks at the borders, of a CTQW distribution. We can identify this behaviour also analytically, using the equation (3.8) that becomes

$$P(n, t) = \frac{1}{3} [J_n^2(kt) + (J_{n-1}(kt) - J_{n+1}(kt))^2]. \quad (3.9)$$

Because of the properties of the Bessel functions, the two quadratic terms have a non negligible contribute during the entire walk. This leads to interference for every momentum states. This result is the starting point for generating the uniform distribution that we need for the search. We will explain the detail in the next chapter.

In the case in figure 3.2, rotating the phase of the first or the third state by π , the

probability is

$$P(n, t) = \frac{1}{3}[J_n^2(kt) + (J_{n-1}(kt) + J_{n+1}(kt))^2] \quad \text{figures 3.2a,3.2b} \quad (3.10)$$

$$P(n, t) = \frac{1}{3}[J_n^2(kt) + (-J_{n-1}(kt) - J_{n+1}(kt))^2] \quad \text{figures 3.2c,3.2d.} \quad (3.11)$$

As we can see the two equations are the same and in fact the probability distribution are equal. We can also notice that the walk is symmetric so the fact that both distributions have the same behaviour, is quite reasonable.

In the latter example for the superposition of three eigenstates, figure 3.3 shows that changing the phase by $\pi/2$ leads to an asymmetric walk. In fact the two probabilities are

$$P(n, t) = \frac{1}{3}[(J_n(kt) + J_{n+1}(kt))^2 + J_{n-1}^2(kt)] \quad \text{figures 3.3a,3.3b} \quad (3.12)$$

$$P(n, t) = \frac{1}{3}[(J_n(kt) - J_{n-1}(kt))^2 + J_{n+1}^2(kt)] \quad \text{figures 3.3c,3.3d} \quad (3.13)$$

that are not equal. Due to the symmetries of the Bessel functions, the left or the right part is suppressed generating a biased walk.

All this theory can be extended for any number of eigenstates. For instance, with a superposition of 5 eigenstates, we have

$$\psi(\theta) = \frac{1}{\sqrt{5}} \frac{1}{\sqrt{2\pi}} (C_{-2} |-2\rangle + C_{-1} |-1\rangle + C_0 |0\rangle + C_1 |1\rangle + C_2 |2\rangle). \quad (3.14)$$

The procedure to calculate the PDF is exactly the same to the one explained in section 3.1. The only difference is that, in this case, we will have more interferences generated by neighbour momentum states. Figure 3.4 shows an example distribution with a superposition of 5 eigenstates. We can distinguish the two peak at the edges but they are almost half of the peaks in the cases with *three* eigenstates. This difference of probability is moved towards the centre where we can see strong interferences the between momentum states.

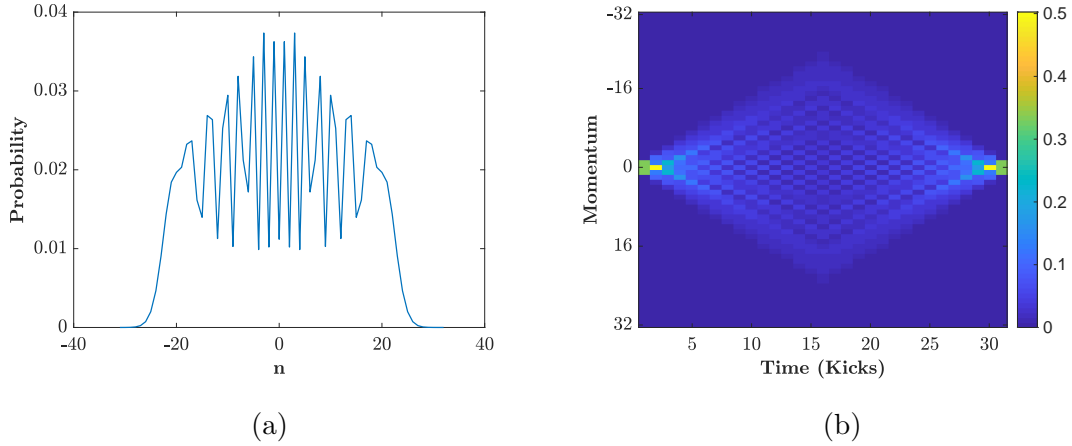


Figure 3.1: PDF vs. momentum eigenstates after 15 kicks (on the left); matrix of the evolution of the PDF VS time (on the right), for the initial state $\psi(0) = (\dots 0 \ 1 \ 1 \ 1 \ 0 \dots)$

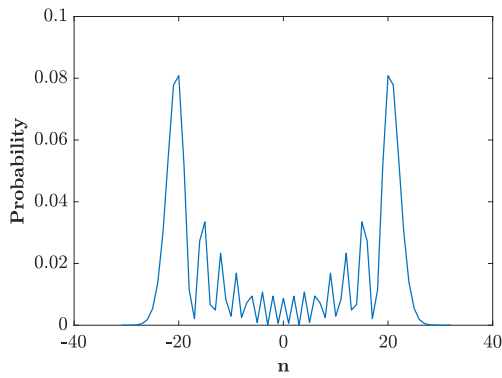
3.2 Superposition in CTQW

In this section we follow the same approach seen in section 3.1 for the QKR, to extend the theory of the CTQW in [8] to the case of linear combination of eigenstates. So let us consider an initial state built with a superposition of *three* eigenstates

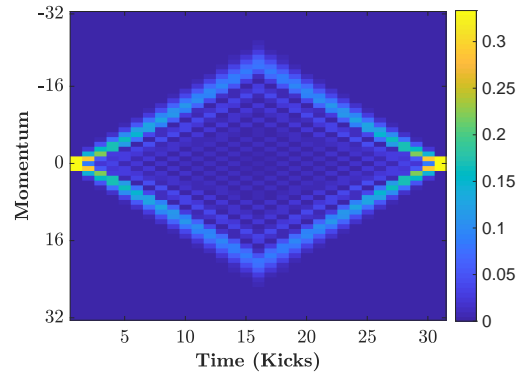
$$|\psi(0)\rangle = \frac{1}{\sqrt{3}} (C_{-1} |-1\rangle + C_0 |0\rangle + C_1 |1\rangle) \quad (3.15)$$

where we used the prefactors C_n as in the case of the QKR in section 3.1. The evolution operator is represented by the equation (2.14), therefore

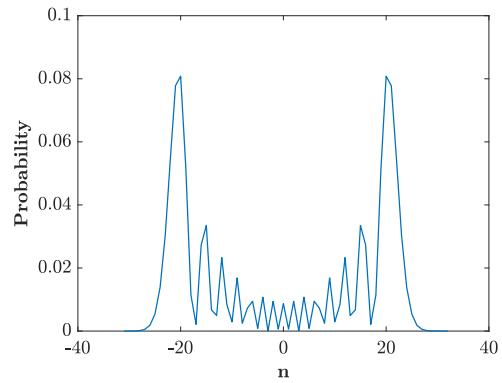
$$\begin{aligned} |\psi(t)\rangle &= U(t) |\psi(0)\rangle = \frac{e^{-iH_\gamma t}}{\sqrt{3}} (C_{-1} |-1\rangle + C_0 |0\rangle + C_1 |1\rangle) \\ &= \frac{1}{\sqrt{3}} \sum_{k=0}^{+\infty} \frac{(-iH_\gamma t)^k}{k!} (C_{-1} |-1\rangle + C_0 |0\rangle + C_1 |1\rangle) \\ &= \frac{1}{\sqrt{3}} \sum_{k=0}^{+\infty} \frac{(-it)^k}{k!} (C_{-1} H_\gamma^k |-1\rangle + C_0 H_\gamma^k |0\rangle + C_1 H_\gamma^k |1\rangle) \end{aligned} \quad (3.16)$$



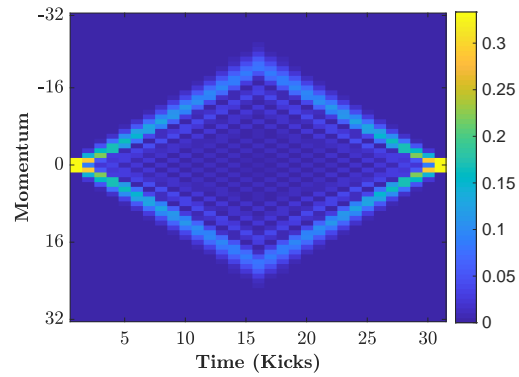
(a)



(b)

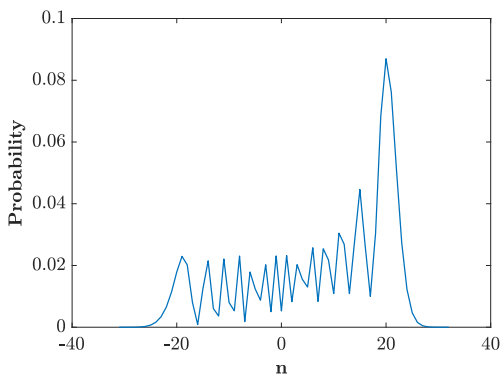


(c)

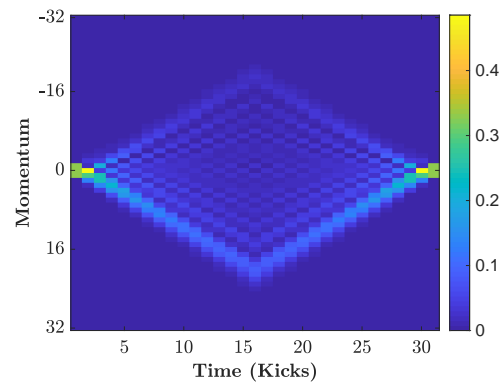


(d)

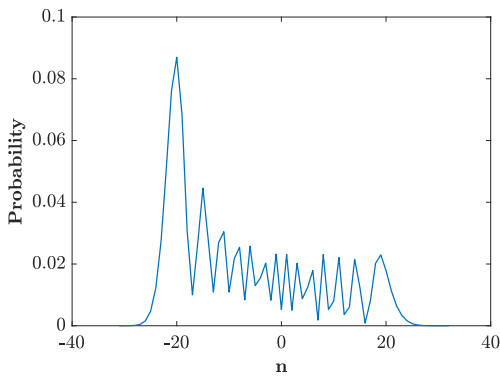
Figure 3.2: PDF vs. momentum eigenstates after 15 kicks (on the left); matrix of the evolution of the PDF VS time (on the right), for the initial state (a)(b) $\psi(0) = (\dots 0 -1 1 1 0 \dots)$; (c)(d) $\psi(0) = (\dots 0 1 1 -1 0 \dots)$



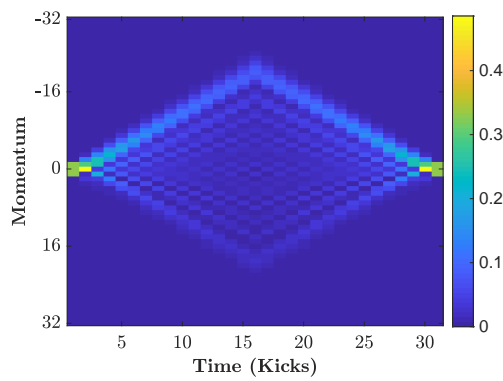
(a)



(b)



(c)



(d)

Figure 3.3: PDF vs. momentum eigenstates after 15 kicks (on the left); matrix of the evolution of the PDF VS time (on the right), for the initial state (a)(b) $\psi(0) = (\dots 0 \ i \ 1 \ 1 \ 0 \ \dots)$; (c)(d) $\psi(0) = (\dots 0 \ 1 \ 1 \ i \ 0 \ \dots)$

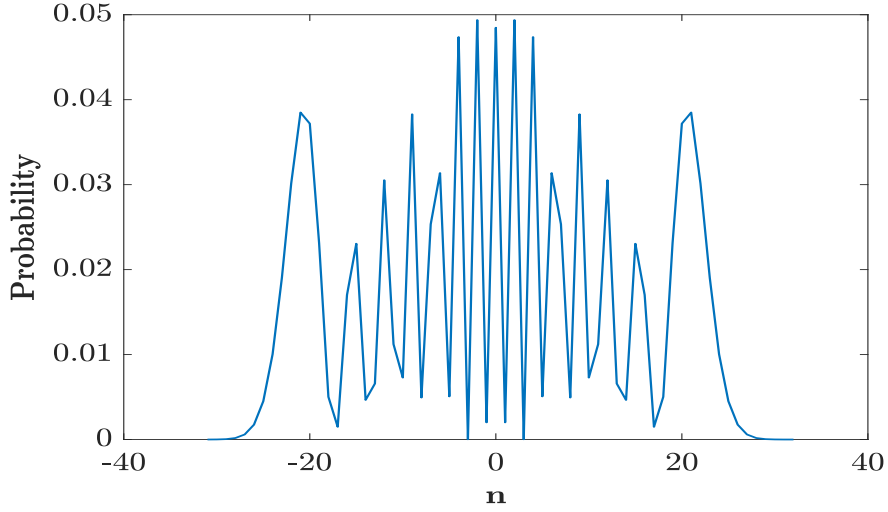


Figure 3.4: PDF vs. eigenstates after 15 kicks for initial state $\psi(0) = (\dots 0 1 1 1 -1 1 0 \dots)$

now we can use the definition (2.19) of the operator H_γ^t

$$\begin{aligned}
&= \frac{1}{\sqrt{3}} \sum_{k=0}^{+\infty} \frac{(-it)^k}{k!} \left(C_{-1} \gamma^k \sum_{n=-k}^k (-1)^k \binom{2k}{k-n} |n-1\rangle + \right. \\
&\quad \left. + C_0 \gamma^k \sum_{n=-k}^k (-1)^k \binom{2k}{k-n} |n\rangle + C_1 \gamma^k \sum_{n=-k}^k (-1)^k \binom{2k}{k-n} |n+1\rangle \right). \tag{3.17}
\end{aligned}$$

At this point, we can multiply every term and switch the summations as explained in section 2.2. Thus we get

$$\begin{aligned}
|\psi(t)\rangle &= \frac{1}{\sqrt{3}} \left(C_{-1} \sum_{n=-\infty}^{+\infty} \sum_{k=|n|}^{\infty} \frac{(-i\gamma t)^k}{k!} (-1)^{|n|} \binom{2k}{k-n} |n-1\rangle + \right. \\
&\quad \left. + C_0 \sum_{n=-\infty}^{+\infty} \sum_{k=|n|}^{\infty} \frac{(-i\gamma t)^k}{k!} (-1)^{|n|} \binom{2k}{k-n} |n\rangle + \right. \\
&\quad \left. + C_1 \sum_{n=-\infty}^{+\infty} \sum_{k=|n|}^{\infty} \frac{(-i\gamma t)^k}{k!} (-1)^{|n|} \binom{2k}{k-n} |n+1\rangle \right). \tag{3.18}
\end{aligned}$$

Here we can change variable in the first and in the last summation: $n' = n - 1$ and $n' = n + 1$. Let us call then $n' = n$ in order to have a simpler notation. After that,

Bessel function identity (2.22) is used, obtaining

$$\begin{aligned}
|\psi(t)\rangle = \frac{1}{\sqrt{3}} & \left(C_{-1} \sum_{n=-\infty}^{+\infty} e^{i\frac{\pi}{2}|n+1|-2i\gamma t} J_{|n+1|}(2\gamma t) |n\rangle + \right. \\
& + C_0 \sum_{n=-\infty}^{+\infty} e^{i\frac{\pi}{2}|n|-2i\gamma t} J_{|n|}(2\gamma t) |n\rangle + \\
& \left. + C_1 \sum_{n=-\infty}^{+\infty} e^{i\frac{\pi}{2}|n-1|-2i\gamma t} J_{|n-1|}(2\gamma t) |n\rangle \right). \tag{3.19}
\end{aligned}$$

We can rewrite the latter equation as

$$\begin{aligned}
|\psi(t)\rangle = \frac{e^{-2i\gamma t}}{\sqrt{3}} & \sum_{n=-\infty}^{\infty} \left(C_{-1} e^{i\frac{\pi}{2}|n+1|} J_{|n+1|}(2\gamma t) + \right. \\
& + C_0 e^{i\frac{\pi}{2}|n|} J_{|n|}(2\gamma t) + \\
& \left. + C_1 e^{i\frac{\pi}{2}|n-1|} J_{|n-1|}(2\gamma t) \right) |n\rangle. \tag{3.20}
\end{aligned}$$

So if we take, for instance, the case for $n > 0$, then we can evaluate the probability as in the section 3.2, which is

$$\begin{aligned}
P_\gamma(n, t) = |\langle n|\psi(t)\rangle|^2 = \frac{1}{3} & \{ J_n^2(2\gamma t) + J_{n-1}^2(2\gamma t) + J_{n+1}^2(2\gamma t) + \\
& - 2\Re[iC_0^* J_n(2\gamma t)(C_1 J_{n-1}(2\gamma t) - C_{-1} J_{n+1}(2\gamma t))] + \\
& - 2\Re[C_{-1}^* C_1 J_{n-1}(2\gamma t) J_{n+1}(2\gamma t)] \}. \tag{3.21}
\end{aligned}$$

This probability is very similar to the equation (3.8) except for a phase of π in the fourth term. This means that a biased walk will have the opposite direction with respect to the one in figure 3.3. However we can solve this issue, for instance, by adding a phase of π to the prefactor C_0 or by implementing kicks with a negative strength $k = -2\gamma$. This can be experimentally done in setups with cold atoms as in Ref. [13], for instance, since in that case k is proportional to the squared Rabi frequency and to the duration of the kick pulse, which are positive, but inversely proportional to the detuning from the atomic transition, which can have also negative value instead. For broader initial states, this generalizes to produce the same evolution as the QKR from the previous subsection.

3.3 Extension to general initial state

In this section, we discuss a more general argument for the equivalence between the QKR and the CTQW described in sec. 2. We first notice that the QKR's evolution operator at quantum resonance of equation (2.7) after t kicks can be formally interpreted as being generated by a Hamiltonian $\mathcal{H} = k \cos \hat{\theta}$ acting continuously for time t . This obviously is true only when one looks at the resulting dynamics for integer t , when the kick occurs. On the basis of momentum eigenstates, the Hamiltonian \mathcal{H} has matrix elements

$$\begin{aligned} \langle m | \mathcal{H} | n \rangle &= \int_0^{2\pi} \frac{e^{-im\theta}}{\sqrt{2\pi}} k \cos \theta \frac{e^{in\theta}}{\sqrt{2\pi}} d\theta \\ &= \frac{k}{2\pi} \int_0^{2\pi} \cos \theta e^{i(n-m)\theta} d\theta \\ &= \begin{cases} k/2 & \text{if } m = n \pm 1 \\ 0 & \text{otherwise} \end{cases} \end{aligned} \quad (3.22)$$

Comparing Eq.s (2.17) and (3.22), we thus see that, if we choose $k = 2\gamma$, the following relation holds for the CTQW Hamiltonian H_γ and the “effective” kick Hamiltonian \mathcal{H} :

$$H_\gamma = 2\gamma \mathbb{I} - \mathcal{H}, \quad (3.23)$$

where \mathbb{I} is the identity matrix over the whole walker's space. Let us now focus on the probability of being in the n -th momentum eigenstate, given *whatever* initial state $|\Psi_0\rangle$ after t kicks of our QKR,

$$P(n, t) = \left| \langle n | \hat{U}^t | \Psi_0 \rangle \right|^2 = \left| \langle n | e^{-i\mathcal{H}t} | \Psi_0 \rangle \right|^2, \quad (3.24)$$

The probability $P_\gamma(n, t)$ that the CTQW starting from the same state in the walker's space leads to the same momentum eigenstate is then, for $\gamma = k/2$ and using Eq.s (3.23)

and (3.24),

$$\begin{aligned}
P_\gamma(n, t) &= |\langle n | e^{-iH_\gamma t} | \Psi_0 \rangle|^2 \\
&= |\langle n | e^{-i(2\gamma\mathbb{I} - \mathcal{H})t} | \Psi_0 \rangle|^2 \\
&= |\langle n | e^{-2i\gamma t} e^{i\mathcal{H}t} | \Psi_0 \rangle|^2 \\
&= |\langle n | e^{i\mathcal{H}t} | \Psi_0 \rangle|^2 \\
&= P(n, -t)
\end{aligned}$$

Therefore, choosing $\gamma = k/2$ as done in the main text, produces a CTQW with time-reversed probability distribution with respect to the evolution induced by the QKR, independently from the initial condition. This is the reason behind the different phase terms discussed in sec. 3.2, as can be verified by changing $t \rightarrow -t$ in Eq. (3.21), which then leads exactly to Eq. (3.8). If $k = -2\gamma$ is chosen instead, the two probability distributions would be equal. In this condition, since the two evolutions are the same, all the theory related to the CTQW can be applied to the QKR and therefore to a realistic working system.

Chapter 4

Quantum Search

Searching for an element in an unsorted database is a well known and well studied problem. If we solve it with classical algorithms, the complexity is of the order of N , the number of elements. While using quantum algorithms, the complexity can be reduced to the order of $O(\sqrt{N})$ [12].

Following the algorithm presented in [12] using the δ -Kicked Rotor (QKR) could be a non trivial task. For this reason, in this chapter we will try to implement a slightly different idea of quantum search using the QKR. Since we are dealing with an experimental quantum system, the problem has interest not only from the point of view of the algorithm, but also from a physical point of view in controlling a realistic Continuous-Time Quantum Walk (CTQW).

4.1 Searching Problem

Let us consider an unsorted database of N elements, where $N = 2^m$ and m is a positive integer. Suppose that we have a function f with domain $\{0, \dots, N - 1\}$ and image

$$f(n) = \begin{cases} 1, & \text{if } n = n_0 \\ 0, & \text{otherwise.} \end{cases} \quad (4.1)$$

The function returns 1 only for the element n_0 , that we will call *target element* or *marked element*, and 0 for all the other points. The problem is to find the point in the domain that has image 1 by calling the function f as many times as we need. Function f is called *oracle* or *black box*.

The general idea is that someone marks an element and we have to find it by querying the oracle. In quantum mechanics the functions are represented by operators in Hilbert space, so we need an operator that marks the state n_0 that we will find successively.

A famous quantum algorithm for a search is the *Grover's algorithm*, ref. chapter 4 in [8] or the original paper in [12]. There is a standard method to construct a unitary operator that implements a generic function. The quantum computer must have two registers. The first stores the domain points and the second stores the image points. Given this, the operator, that we will call \mathcal{R}_f , can be described by the following relation

$$\mathcal{R}_f |n\rangle |i\rangle = |n\rangle |i \oplus f(n)\rangle \quad (4.2)$$

where \oplus is the *binary sum* or *bitwise xor*. The standard method is: repeat the value of x to guarantee reversibility and perform the binary sum of the image of x with the value of the second register. For any function f , the resulting operator will be unitary. The first register refers to space of the domain, so it has dimension N . While the second register refers to the space of the image point that can be 0 or 1, so it has dimension 2. For instance, if the state of the second register is $|0\rangle$, the action of \mathcal{R}_f is

$$\mathcal{R}_f |x\rangle |0\rangle = \begin{cases} |n_0\rangle |1\rangle, & \text{if } n = n_0 \\ |n\rangle |0\rangle, & \text{otherwise.} \end{cases} \quad (4.3)$$

Grover's algorithm uses another operator, that we will call R_D , defined by

$$\mathcal{R}_D = (2|D\rangle\langle D| - I_N) \otimes I_2 \quad (4.4)$$

where I_N and I_2 are identity matrices respectively of dimension $N \times N$ and 2×2 , \otimes is the tensor product and $|D\rangle$ is the diagonal state defined as

$$|D\rangle = \frac{1}{\sqrt{N}} \sum_{n=0}^{N-1} |n\rangle. \quad (4.5)$$

So the the evolution operator that perform one step of the algorithm is

$$U = \mathcal{R}_D \mathcal{R}_f. \quad (4.6)$$

The algorithm states that if we apply the operator U recursively $\lfloor \frac{\pi}{4} \sqrt{N} \rfloor$ times, when we measure the first register, we will find x_0 with probability $1 - \frac{1}{N}$ [8].

4.2 Search algorithm using QKR

In the most of search algorithms, the initial state is the state $|D\rangle$, defined in the equation (4.5), which is the superposition of all the eigenstates of the system. However if we want to use the Grover's algorithm with the QKR we should modify the Hamiltonian in order to implement the operator U in the equation (4.6) and it could not be an easy process. Therefore in this section we will try a different approach to search an element in an unsorted database.

The idea of searching an element using QKR, is to mark a state after applying the operator U t times, and then to go back with U^\dagger applied t times as well. As seen in the section 3.1.1, we use 15 kicks for the forward evolution and other 15 kicks for the backward. Therefore, to realize a search with the QKR, we should have uniform distribution after 15 kicks. However this is not possible because of the oscillations generated by the evolution of the system, which is described by the Hamiltonian in the equation (2.1). The closest distribution to the uniform one that we can achieve, can be found numerically and it is shown in figure 4.1a. For the purpose, we defined an error function *err*

$$err(\mathbf{C}) = \sum_{n=-N/2}^{N/2} |P(n, t, \mathbf{C}) - u(n)|^2, \quad (4.7)$$

where N is the width of the distribution in terms of the number of the eigenstates, $\mathbf{C} = \{C_{-1}, C_0, C_1\}$ is the vector of the initial coefficients, $P(n, t)$ is the probability distribution as in the equation (3.8) with $t = 15$, $u(n)$ is an uniform distribution, constant over an interval of width N . Given this, we found the coefficients C_1, C_{-1}, C_0 such that

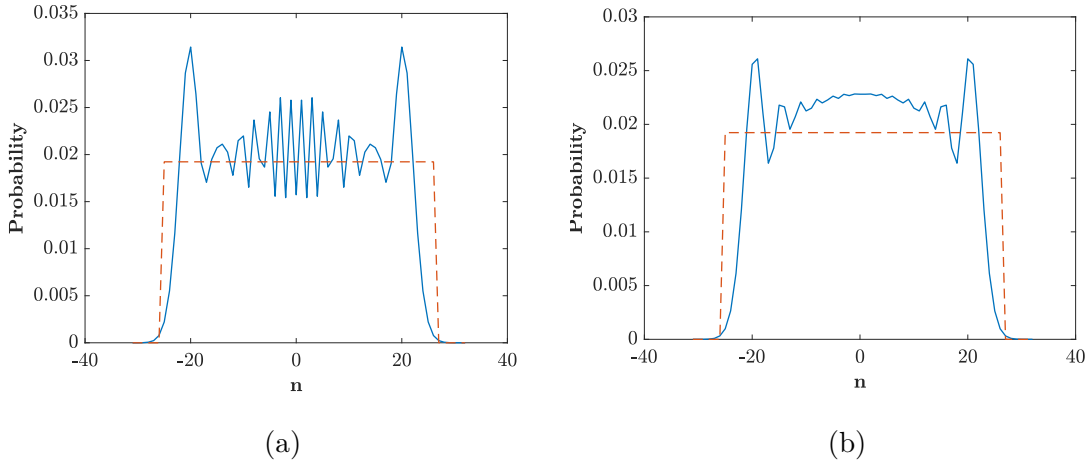


Figure 4.1: (a) Probability Density Function (PDF) vs. momentum eigenstates after 15 kicks for initial state centred around 0 $\psi(0) = (\dots 0, 0.48, 0.73, 0.48, 0\dots)$ (solid line); (b) PDF vs. momentum eigenstates after 15 kicks for initial state centred around 0 $\psi(0) = (\dots 0, 0.229, 0.669, 0.669, 0.229, 0\dots)$ (solid line). Both the distribution are compared with the flat one (dashed line) used for the optimization.

err is minimum and we obtained $C_{-1} = 0.48, C_0 = 0.73, C_1 = 0.48$. Alternatively we can also use the initial state with *four* coefficients, obtaining the result in figure 4.1b. We can achieve a more flat distribution even though the width is the same of the case with three coefficients.

After 15 kicks we mark an element that, as example, we choose $\frac{N}{2} + 5$. The marking operation consists in adding a phase of π to the state that we want to find and leaving the others unchanged. So the operator will be diagonal with all 1's except for the column $\frac{N}{2} + 5$, in which the phase factor is applied. In formula we have

$$P = \begin{bmatrix} 1 & 0 & \dots & 0 & \dots & 0 \\ 0 & 1 & \dots & 0 & \dots & 0 \\ \vdots & \vdots & \ddots & \vdots & \vdots & \vdots \\ 0 & 0 & \dots & e^{i\pi} & \dots & 0 \\ \vdots & \vdots & \dots & \vdots & \ddots & \vdots \\ 0 & 0 & \dots & 0 & \dots & 1 \end{bmatrix}. \quad (4.8)$$

Figure 4.2b shows the marking moment which is at $t = 15$. From that point on,

a new walk is created starting from the marked state. This walk presents the same characteristics of the one in figure 3.2a which has the two peaks at the edges. In fact, in the figure 4.2a we can see part of the initial state in the middle and two little peaks at the borders. Our goal is to study the walk generated by the marked state, so we would like to eliminate the central peak namely the initial state. This operation is not so simple because, experimentally, it is difficult to suppress only some momentum eigenstates while keeping the evolution of the rest coherent. However one could try to adapt Raman transitions to eliminate a specific momentum class by changing the internal state of the atoms [14]. If this were possible, the result will be very similar to the one in figure 4.4a. In particular the figure shows that, without the interference of the initial state, only the walk generated by the marked state is propagated.

Instead of directly suppressing the initial state, which can be difficult due to the experimental limits, another possibility could be the numerical processing after measuring the state of the system. Since we know the initial distribution, the idea in this case is to subtract the PDF of the initial state from the distribution that we get after 30 kicks, which is the one in figure 4.2a. The subtraction between those PDFs will generate negative values of probability. However we can plot only the points with probability greater than 0 and set the others to 0. Figure 4.4b shows the resulting distribution which is equal to the one in figure 4.4a. This equality between the distributions obtained with two different approaches, may be a further indication on the correctness of the result. Various experiments on QKR have been realized with different techniques, such as using cold atoms [15, 16] or, more recently, Bose Einstein Condensate (BEC) [17, 18]. In both cases scientists used optical signal as information medium. For this reason it is important to have the quantity called *Signal-to-Noise ratio* (SNR), which is the ratio between the power of the signal and the power on the noise, as high as possible in order to obtain an high quality signal. Comparing the SNRs between experiments with cold atoms and those with BEC, it turns out that the first kind of experiments has worse SNR than the second.

At this point in order to find the marked state, we can notice that the walk generated

by the marked state is exactly centred around it. Given this, we can adopt two different strategies to recover the marked element from the probability distribution of the walk. Hence, the probabilities in the peaks of interest, must be sufficiently above the SNR, in order to distinguish them from the usually dominating centre in the protocol.

Method 1 The first strategy exploits the position of the two highest peaks. If we consider the figure 4.4a we can read the position corresponding to the two peaks and find the value of the state n_0 by

$$n_0 = n_\ell + \frac{n_r - n_\ell}{2}, \quad (4.9)$$

where n_ℓ and n_r are the eigenvalues corresponding to the left and the right peak respectively. In the our case we have $n_\ell = -15$, $n_r = 25$ so $n_0 = -15 + \frac{40}{2} = 5$ as expected.

Sometimes it can happen that one peak is cut off when we remove the initial state. This problem occurs if the marked state is at the boundary of the distribution, for instance $n_0 = 20$, as figure 4.3a shows. Only for this simulation, in order to visualize the entire walk, we needed to enlarge the momentum space from 64 to 128 eigenvalues.

In this case, to find the marked state, we can exploit the fact that the distribution is completely symmetric and it has a constant width once the parameters k and t are set. The width that we consider is the distance between the two highest peaks. In particular for the values of k and t that we chose, the width is 40. So given that the position of the visible peak is $n_r = 40$, the suppressed peak would be at the state $n_\ell = 0$. At this point we can evaluate the value of the state n_0 using the equation (4.9). The result is 20, as expected.

Alternatively we can use this approach to directly evaluate the position n_0 , even if we have both the peaks, just by using one of them. If we choose the right peak we get

$$n_0 = n_r - \frac{d}{2}, \quad (4.10)$$

where d is the distance between the peaks. In the last example that we considered, $n_r = 40$, $d = 40$ then $n_0 = 20$. Otherwise if we choose the left peak, we have to sum

the half of the width

$$n_0 = n_\ell + \frac{d}{2}. \quad (4.11)$$

Thus we have $n_\ell = 0$, $d = 40$ and then $n_0 = 20$.

Method 2 Another way to find the marked state can be followed. If we apply again 15 kicks with the operator U defined in the equation (2.7), the walk converges to the marked state. The result is shown in figure 4.5. However this method can be performed only if we are able to eliminate the initial state after 30 kicks. In fact if we can do so, the PDF at $t = 45$ is a peak centred on the state that we were searching, as figure 4.5a shows. While if we can not remove the initial state, after 45 kicks we will have interference between the distribution in figure 4.1a and the one in figure 4.5a, and we will not be able to recover the target element so easily.

Even using this method we can run across the problem seen in the method 1. However, as figure 4.3b shows, we can still recover the marked state after 45 kicks.

The signal in this case is very low, so it important, as discussed above, to have a value of SNR sufficiently large in order to distinguish the peak from the noise.

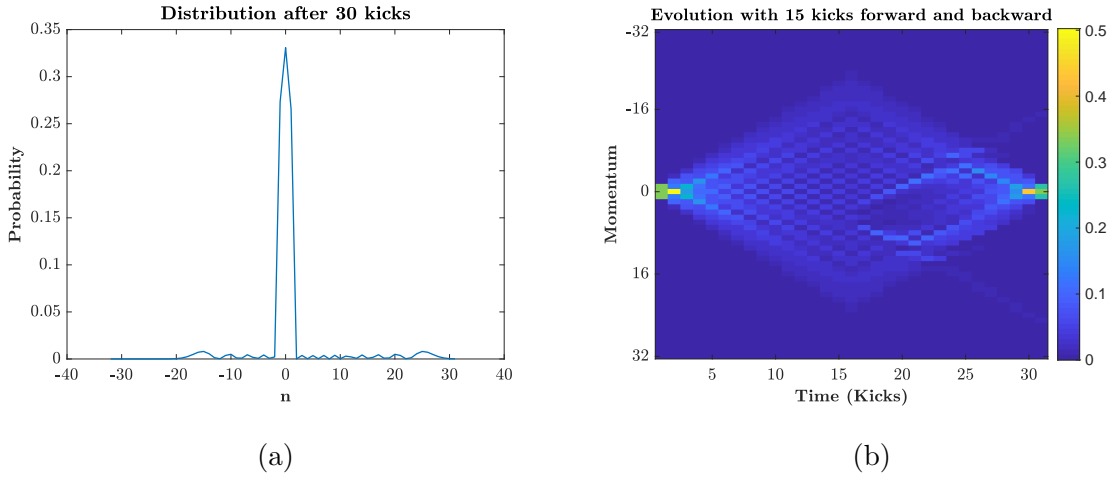


Figure 4.2: (a) Distribution vs. momentum at $t = 30$; (b) Forward evolution of the only initial distribution for 15 kicks and backward evolution with also the marked element $\frac{N}{2} + 5$

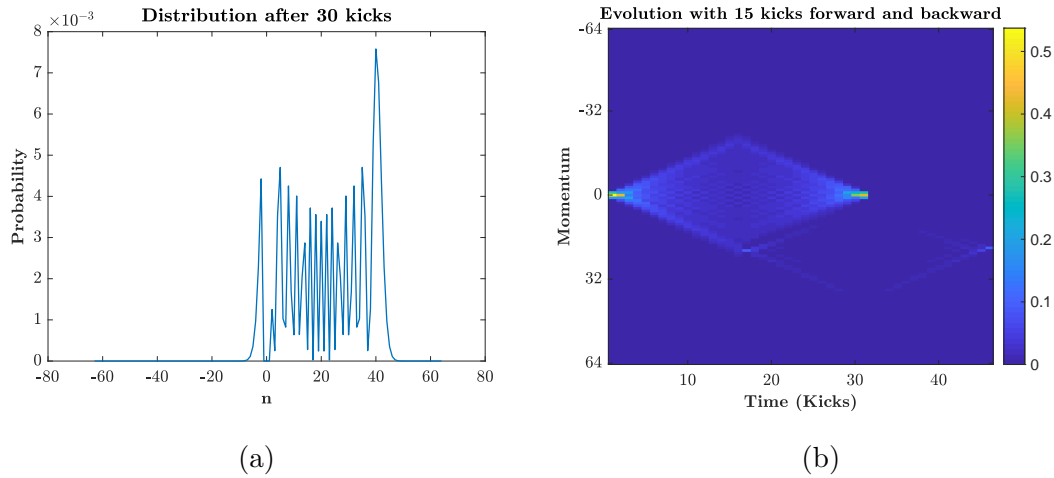


Figure 4.3: (a) Probability distribution vs. momentum after 30 kicks for the marked state $n_0 = 20$; (b) Same as the figure 4.2b for the first 30 kicks then other 15 forward kicks are applied to let the walk converges to the marked element.

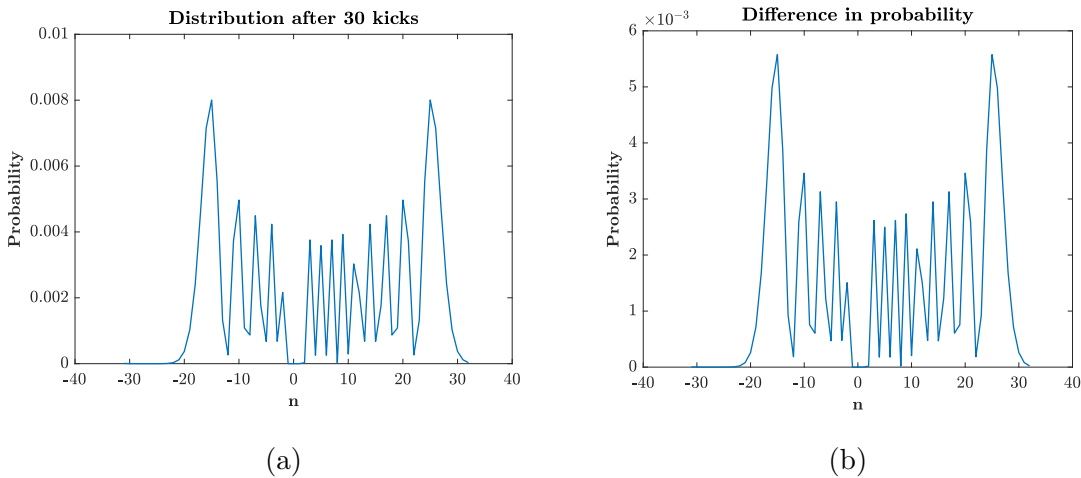


Figure 4.4: (a) Probability distribution vs. momentum after 30 kicks obtained if it were possible to remove the initial state with the Raman transition; (b) Probability distribution vs. momentum after 30 kicks obtained from the difference between the distribution in figure 4.2a and the initial one.

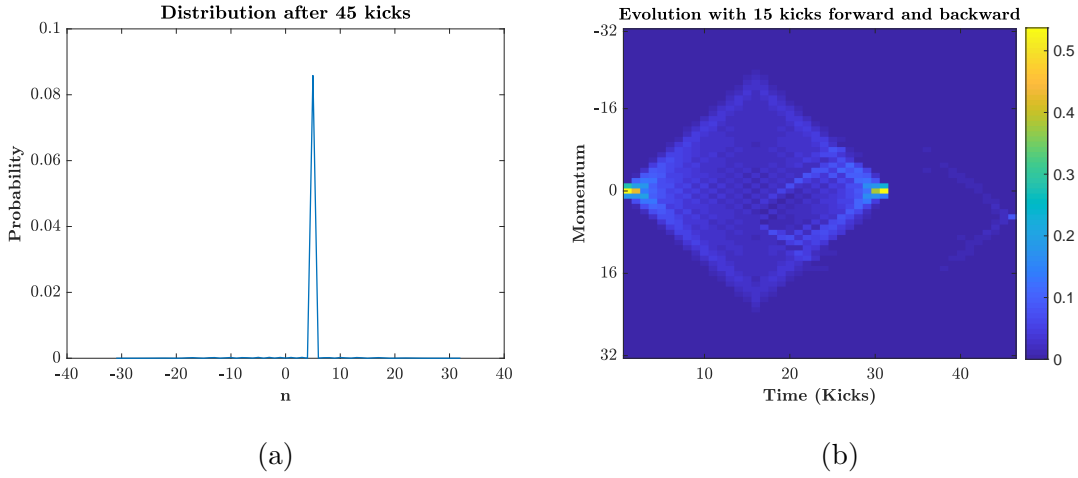


Figure 4.5: (a) Distribution vs. momentum after $t = 45$ kicks; (b) Same as the figure 4.2b for the first 30 kicks then other forward 15 kicks are applied to let the walk converges to the marked element.

4.2.1 Performance

The width of the distribution of the walk changes according to the parameters k and t . So it is natural to ask what the expected distance is from the origin induced by the probability distribution. It is important to determine how far away from the origin we can find the particle as time, or kicks, goes on. The expected distance is a statistical quantity that captures this idea and is equal to the *position standard deviation* when the probability distribution is symmetrical. The Standard Deviation (STD) $\sigma(t)$ is defined as

$$\sigma(t) = \sqrt{\langle n^2 \rangle - \langle n \rangle^2}, \quad (4.12)$$

where $\langle n^2 \rangle$ is the mean square value and $\langle n \rangle$ is the expected position.

Since the distribution is symmetrical, we know that the expected position is

$$\langle n \rangle = \sum_{n=-\infty}^{\infty} n p(n, t) = 0, \quad (4.13)$$

where $p(n, t)$ is the walker's distribution. Given this, the equation (4.12) becomes

$$\sigma(t) = \sqrt{\sum_{n=-\infty}^{\infty} n^2 p(n, t)}. \quad (4.14)$$

In the case of quantum walk, in particular of the QKR, the symmetric probability distribution of the momentum eigenstates expands ballistically around its initial value. This means that the STD is proportional to the number of kicks [19, 20]. The classical random walk, instead, has a probability distribution which is approximately Gaussian and it is defined as follows [8]

$$p(n, t) \simeq \frac{2}{\sqrt{2\pi t}} e^{-\frac{n^2}{2t}}. \quad (4.15)$$

Figure 4.6a shows a comparison between the STD of the CTQW (solid line) and the one of a classical random walk (dashed line). The first one is obtained using the walker's distribution generated by a single initial state [equation (2.13)], while the second is obtained from the equation (4.15). Both the standard deviations have been evaluated considering values of t from 1 to 100. As we can see from the figure, the STD of the CTQW is linear and proportional to the number of the kicks t . More precisely we can evaluate the slope of the straight line, obtaining $\sigma(t) = 0.93t$. The STD of the classical random walk, instead, is proportional to the \sqrt{t} , so the expansion is slower than the one of the CTQW.

Figure 4.6b shows, instead, the comparison between the STD of the distribution, that we use for the search, obtained from the minimization of the error function explained in the section 4.2, and the STD of the classical random walk. From the figure we can notice that the behaviour of the functions is the same of the one in the figure 4.6a. The only difference is that this simulation stopped at $t = 15$ which is the time of the maximum extension of the distribution that we use for the search.

At this point, if we consider the number of kicks as defining the complexity of the algorithm, we can say that the CTQW has a quadratic gain with respect to the classical random walk. This means that, in order to reach a state far away from the

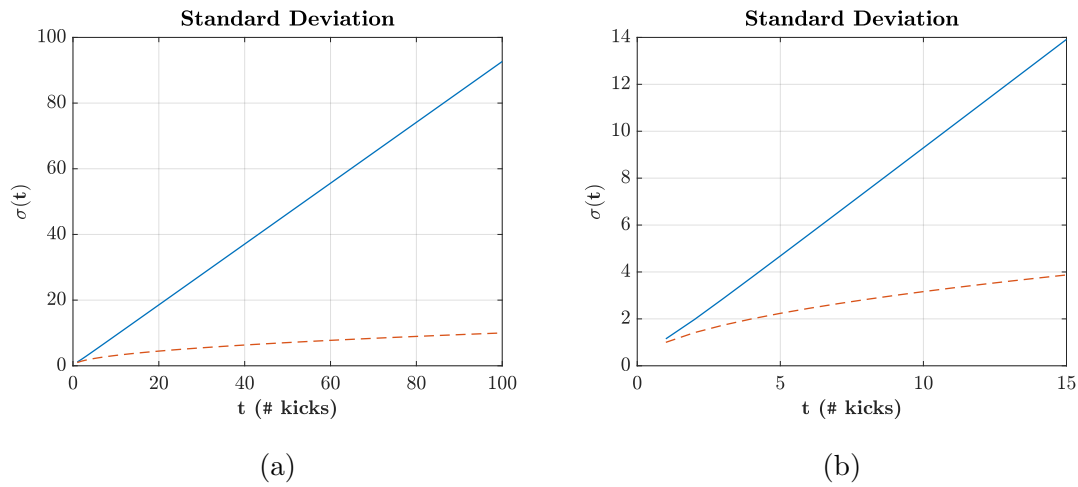


Figure 4.6: STD of CTQW generated by the QKR (solid line) and STD of classical random walk (dashed line), for the distribution in the equation (2.13) with $t \in [1, 100]$ (a), and the one in the equation (3.8) with $t \in [1, 15]$ (b). In both the figures, equation (4.15) has been used for the STD of classical random walk.

starting point using the CTQW of the QKR, we need a number of steps smaller than the classical random walk.

Since k is an optimal value for the experiments, we could only improve the performance increasing the number of kicks. However, if we increase too much the value of t , the distribution will spread and overall take on very small values. Consequently we could not be able to manage the signal anymore due to the experimental noise. Therefore we need to find a trade-off value of t that allows to improve the performance without losing too much of the signal in a realistic experiment.

Chapter 5

Conclusions and future developments

5.1 Conclusions

We have seen that a quantum system used in the Chaos Theory, that is the δ -Kicked Rotor (QKR) in resonance conditions, has the evolution which is completely identical to the one of the Continuous-Time Quantum Walk (CTQW). In particular we have shown analytically that, for the case of a single initial state, the probability distribution of the momentum eigenstates of the QKR correspond to the distribution of a walker in the CTQW. Since the aim of the work was to find a possible quantum search protocol, we have extended the result of the chapter 2 to the case of an initial state obtained from the superposition of *three* momentum eigenstates. What we obtained were three different distributions according to the values of the coefficients used for building the linear combination of the initial state. In detail we have seen that we can control the bias of the walk simply by rotating the coefficients C_1 or C_{-1} , in the equation (3.3), by a phase of $\pi/2$. All the results were supported by the theoretical analysis that perfectly corresponds with the numerical simulations. Moreover we have used the same approach to extend the theory of CTQW according to the definition of Portugal's book. From

the latter result, we have seen that the walker's distribution of the CTQW for three states differ by a phase of π from the momentum distribution of QKR. This issue can be solved by rotating the coefficient C_0 by π or by using negative kick strength for the QKR [13]. We also argued in sec. 3.3 that our results extend to arbitrary initial states.

In the fourth and last chapter, we have implemented a protocol for the quantum walk using the experimental CTQW. First of all we have numerically evaluated the optimally broad (closest to uniform) distribution that can be obtained with the linear combination of three eigenstates after 15 kicks. From such numerical optimization we obtained the distribution in figure 4.1a in the momentum space. As second step we marked a state, according to the theory of the Grover's algorithm for quantum search, by rotating its phase by π . We noticed that the marked element created a walk starting from the marked position. Therefore our aim was to recover the state that we would to find. For the purpose we proposed two methods: the first numerically, by evaluating the position of the peaks and applying the formula (4.9); the second consists in applying further 15 kicks with the operator in the equation (2.7). However both the methods are constraint to the suppression of the initial state. If we cannot "remove" the initial state in some way, we cannot apply either of the two methods. Even for this issue, two solutions have been presented. The first approach can be done directly in the experiment and uses the Raman transitions to remove the initial state. The second, instead, is a numerical approach and consists in subtracting the distribution obtained after 15 kicks with the initial one. Both the alternatives can be followed but we have to deal with the experimental problems to guarantee the detection of the wanted smallest peaks. Nevertheless, recent experiments with BEC have shown better signal with respect to the old ones [17, 18].

Finally the comparison of the performance of the classical and the quantum walk is made. The complexity of the algorithms has been evaluated in terms of the number of applied kicks. The benchmark that we chose is the standard deviation that define the width of the distribution. From the results we have seen that the quantum walk has a quadratic gain with respect to the classical one. Further improvement of the

performance can be done only by increasing the number of kicks but we still need to pay attention to the experimental noise.

5.2 Future developments

Future works can be realised in order to build more efficient experimental CTQW. In this thesis we have implemented a CTQW on a line, therefore a quite natural improvement could be the implementation of a multidimensional quantum walk. One of the advantages of this new approach is the fact that we can cover more than *two* eigenstates for each kick. For instance, if we consider an infinite bidimensional lattice, every state is connected to other *four* states. Therefore at each step the particle will be split into *four* parts.

During the thesis, for a short time, I also worked on Discrete-Time Quantum Walk (DTQW) still realized with the QKR [21]. Such a discrete variant is quite different from the continuous analogous. In fact its evolution is described by two operators: $U = SC$, where the S represents the shift and C is the coin [8]. However its probability distribution still presents two peaks at the edges, so the performance are very similar to the continuous case. The power of this type of walk, is that we can try to implement new algorithms, such as the original Grover's algorithm, changing only the coin operator. More about this topic, can be found in [8].

Further analysis on the behaviour of the CTQW can be done. For instance the *recurrence probability* can be evaluated. For instance, if the initial state is the state $|0\rangle$, the recurrence probability is the probability that the walker returns to the original state at time t . In the case of the QKR, we can expect that such probability corresponds to $p(0, t) = J_0^2(kt) \sim \frac{2}{\pi kt} \cos^2(kt - \frac{1}{4}\pi)$. The asymptotic approximation is taken from the equation 9.2.1 of [11].

Appendix A

Bessel identity check

Let us consider the case $n > 0$ so the goal is to show that

$$e^{-2i\gamma t} J_n(2\gamma t) = e^{\frac{i\pi n}{2}} \sum_{k=n}^{\infty} \frac{(-i\gamma t)^k}{k!} \binom{2k}{k-n}. \quad (\text{A.1})$$

By changing index k to $\ell = k - n$ we obtain

$$\frac{e^{-2i\gamma t} J_n(2\gamma t)}{e^{\frac{i\pi n}{2}}} = \sum_{\ell=0}^{\infty} \frac{(-i\gamma t)^\ell}{\ell!} \binom{2(\ell+n)}{\ell} \frac{\ell!}{(\ell+n)!} (-i\gamma t)^n. \quad (\text{A.2})$$

Now let us change t to $t' = -i\gamma t$, so we have

$$\frac{e^{2t'} J_n(2it')}{t'^n e^{\frac{i\pi n}{2}}} = \sum_{\ell=0}^{\infty} \binom{2(\ell+n)}{\ell} \frac{\ell!}{(\ell+n)!} \frac{t'^\ell}{\ell!} \quad (\text{A.3})$$

The right part is the Taylor expansion of the left term, so now the goal is to show that

$$e^{-\frac{i\pi n}{2}} \frac{d^\ell}{dt'^\ell} \left(\frac{e^{2t'} J_n(2it')}{t'^n} \right) \Big|_{t'=0} = \frac{\ell!}{(\ell+n)!} \binom{2(\ell+n)}{\ell} \quad (\text{A.4})$$

using the well known expression of the Bessel function

$$J_n(2it') = \sum_{m=0}^{\infty} \frac{(-1)^m}{m!(m+n)!} (it')^{2m+n} \quad (\text{A.5})$$

and the Taylor expansion of the exponential function

$$e^{2t'} = \sum_{p=0}^{\infty} \frac{(2t')^p}{p!}. \quad (\text{A.6})$$

Thus we get

$$\begin{aligned} & e^{-i\frac{\pi}{2}n} \frac{d^\ell}{dt'^\ell} \left(\frac{1}{t'^n} \sum_{p=0}^{\infty} \frac{2^p t'^p}{p!} \sum_{m=0}^{\infty} \frac{(-1)^m i^{2m+n}}{m!(m+n)!} t'^m t'^{2n} \right) \Big|_{t'=0} \\ &= \sum_{m,p=0}^{\infty} \frac{(-1)^m i^{2m+n}}{m!(m+n)!} \frac{2^p}{p!} \frac{d^\ell}{dt'^\ell} (t'^{2m+p}) e^{-i\frac{\pi}{2}n} \Big|_{t'=0} \end{aligned} \quad (\text{A.7})$$

Since we are going to take $t' = 0$, the only terms we have to consider are those such that $2m + p = \ell$. Then

$$\frac{d^\ell}{dt'^\ell} (t'^{2m+p}) \Big|_{t'=0} = \ell! \quad \text{and} \quad 2m + p = \ell \quad (\text{A.8})$$

Finally we have

$$e^{-i\frac{\pi}{2}n} \frac{d^\ell}{dt'^\ell} \left(\frac{e^{2t'} J_n(2it')}{t'^n} \right) \Big|_{t'=0} = \sum_{m=0}^{\infty} \frac{(-1)^m i^{2m+n} 2^{\ell-2m} \ell!}{m!(m+n)!(\ell-2m)!} e^{-i\frac{\pi}{2}n} \quad (\text{A.9})$$

$$= \ell! \sum_{m=0}^{\lfloor \frac{\ell}{2} \rfloor} \frac{2^{\ell-2m}}{m!(m+n)!(\ell-2m)!} \quad (\text{A.10})$$

where we have used the fact that $(-1)^m i^{2m+n} e^{-i\frac{\pi}{2}n} = 1$ and m must be at most $\lfloor \frac{\ell}{2} \rfloor$, being $\lfloor \cdot \rfloor$ the floor function, because the argument of the factorial must be greater or equal to 0. Thus

$$e^{-i\frac{\pi}{2}n} \frac{d^\ell}{dt'^\ell} \left(\frac{e^{2t'} J_n(2it')}{t'^n} \right) \Big|_{t'=0} = \frac{\ell!}{(n+\ell)!} \sum_{m=0}^{\lfloor \frac{\ell}{2} \rfloor} \binom{n+\ell}{m} \binom{n+\ell-m}{\ell-2m} 2^{\ell-2m} \quad (\text{A.11})$$

$$= \frac{\ell!}{(n+\ell)!} \binom{2(n+\ell)}{\ell}. \quad (\text{A.12})$$

The right term of this last equation is equal to the right term of the equation A.4. In the last step we have used the identity that we will prove in the following section.

A.1 Modified Vandermonde's identity

In the equation A.10 we have used a modified version of Vandermonde's identity:

$$\sum_{m=0}^{\lfloor \frac{\ell}{2} \rfloor} \binom{n}{m} \binom{n-m}{\ell-2m} 2^{\ell-2m} = \binom{2n}{\ell}. \quad (\text{A.13})$$

It can be proven in many ways, but we will show the combinatorial one.

Proof. The right part is quite intuitive since it represents the number of subsets of size ℓ in a set of $2n$ elements.

Now I will show a different way to count the subsets of size ℓ which correspond to the left hand side. So let us consider the binary sets defined as $A_i = \{2i - 1, 2i\}$ for $i = 1, 2, \dots, n$ such that we can partition the entire set of size $2n$, $\{1, 2, \dots, 2n\}$. Now, let us define S as the set of subsets of size ℓ from the set $\{1, 2, \dots, 2n\}(\{1, 2, \dots, \ell - 1, \ell\}; \{1, 2, \dots, \ell - 1, \ell + 1\}; \dots)$. We can build any set in S by choosing first m sets A_i from the n for which $|S \cap A_i| = 2$. This choice can be done in $\binom{n}{m}$ possible ways. Then fixed the A_i , we choose $\ell - 2m$ sets from the remaining $n - m$, for which $|S \cap A_i| = 1$ and we have $\binom{n-m}{\ell-2m}$ ways to perform the choice. Moreover, for this last choice, we have other $2^{\ell-2m}$ possible combinations since we are using sets of two elements. Now summing over all the possible values of m , we get the total number of the subsets of size ℓ . \square

Example. Let consider a set of 6 elements $\{1, 2, 3, 4, 5, 6\}$, so $n = 3$, and suppose to have $\ell = 3$. There are $\binom{2n}{\ell} = \binom{6}{3} = 20$ subsets of size 3.

Alternatively let us consider the subsets $S = \{1, 2, 3\}, \{1, 2, 4\}, \{1, 2, 5\} \dots$. To build any set in S we choose first the set of i such that $|S \cap A_i| = 2$ (i.e. $|S \cap A_1| = |\{1, 2\}| = 2, |S \cap A_2| = |\{3, 4\}| = 2, |S \cap A_3| = |\{5, 6\}| = 2$) which can be done in $\binom{3}{1} = 3$ ways. Then, fixed the A_i , we choose from the remaining A_i 's, those such that $|S \cap A_i| = 1$ (e.g. fixed A_1 , we can choose A_2 or A_3 in order to have $|S \cap A_2| = |\{3\}| = 1$ or $|S \cap A_2| = |\{4\}| = 1$ or $|S \cap A_3| = |\{5\}| = 1 \dots$). This last choice can be done in $2^{\ell-2m}$ possible ways since we are using an alphabet of 2 elements. In terms of sets A_i we have: $A_1 A_2^+, A_1 A_2^-, A_1^- A_2^- A_3^-, A_1^- A_2^- A_3^+, \dots$, where A_i^\pm means the even or odd element in A_i . So in the sum, the first binomial takes into account the number of intersection, with the set S , with 2 elements, the second binomial represents the number of intersection with 1 element and $2^{\ell-2m}$ takes into account the parity of the set A_i . In formula:

$$\sum_{m=0}^1 \binom{3}{m} \binom{3-m}{3-2m} 2^{3-2m} = \binom{3}{0} \binom{3}{3} 2^3 + \binom{3}{1} \binom{2}{1} 2^1 = 8 + 12 = 20.$$

Bibliography

- [1] M. Mohseni, P. Read, H. Neven, S. Boixo, V. Denchev, R. Babbush, A. Fowler, V. Smelyanskiy, and J. Martinis, “Commercialize quantum technologies in five years,” *Nature*, vol. 543, p. 171–174, 2017. [Online]. Available: <http://www.nature.com/news/commercialize-quantum-technologies-in-five-years-1.21583>
- [2] D.-W. Company, “<https://www.dwavesys.com/resources/publications?type=technology>,” July 2019.
- [3] D. Bouwmeester, I. Marzoli, G. P. Karman, W. Schleich, and J. P. Woerdman, “Optical galton board,” *Phys. Rev. A*, vol. 61, p. 013410, Dec 1999. [Online]. Available: <https://link.aps.org/doi/10.1103/PhysRevA.61.013410>
- [4] J. Du, H. Li, X. Xu, M. Shi, J. Wu, X. Zhou, and R. Han, “Experimental implementation of the quantum random-walk algorithm,” *Phys. Rev. A*, vol. 67, p. 042316, Apr 2003. [Online]. Available: <https://link.aps.org/doi/10.1103/PhysRevA.67.042316>
- [5] J. A. Izaac, X. Zhan, Z. Bian, K. Wang, J. Li, J. B. Wang, and P. Xue, “Centrality measure based on continuous-time quantum walks and experimental realization,” *Phys. Rev. A*, vol. 95, p. 032318, Mar 2017. [Online]. Available: <https://link.aps.org/doi/10.1103/PhysRevA.95.032318>
- [6] M. Weiß, C. Groiseau, W. K. Lam, R. Burioni, A. Vezzani, G. S. Summy, and S. Wimberger, “Steering random walks with kicked ultracold

- atoms,” *Phys. Rev. A*, vol. 92, p. 033606, Sep 2015. [Online]. Available: <https://link.aps.org/doi/10.1103/PhysRevA.92.033606>
- [7] M. Delvecchio, F. Petiziol, and S. Wimberger, “Equivalence of resonant quantum kicked rotor and one-dimensional continuous-time quantum walk.”
- [8] R. Portugal, *Quantum Walks and Search Algorithms*. Springer, 2013.
- [9] S. Wimberger, I. Guarneri, and S. Fishman, “Quantum resonances and decoherence for δ -kicked atoms,” *Nonlinearity*, vol. 16, no. 4, pp. 1381–1420, 2003.
- [10] J. Ni, W. K. Lam, S. Dadras, M. F. Borunda, S. Wimberger, and G. S. Summy, “Initial-state dependence of a quantum resonance ratchet,” *Physical Review A*, vol. 94, no. 4, pp. 1–6, 2016.
- [11] M. Abramowitz and I. Stegun, *Handbook of Mathematical Functions*. New York: Dover, 1972.
- [12] L. K. Grover, “A Fast quantum mechanical algorithm for database search,” 1996.
- [13] S. Dadras, A. Gresch, C. Groiseau, S. Wimberger, and G. S. Summy, “Quantum Walk in Momentum Space with a Bose-Einstein Condensate,” *Phys. Rev. Lett.*, vol. 121, p. 070402, Aug 2018. [Online]. Available: <https://link.aps.org/doi/10.1103/PhysRevLett.121.070402>
- [14] M. Kasevich, D. S. Weiss, E. Riis, K. Moler, S. Kasapi, and S. Chu, “Atomic velocity selection using stimulated raman transitions,” *Phys. Rev. Lett.*, vol. 66, pp. 2297–2300, May 1991. [Online]. Available: <https://link.aps.org/doi/10.1103/PhysRevLett.66.2297>
- [15] M. B. d’Arcy, R. M. Godun, M. K. Oberthaler, D. Cassettari, and G. S. Summy, “Quantum enhancement of momentum diffusion in the delta-kicked rotor,” *Phys. Rev. Lett.*, vol. 87, p. 074102, Jul 2001. [Online]. Available: <https://link.aps.org/doi/10.1103/PhysRevLett.87.074102>

-
- [16] M. B. d’Arcy, R. M. Godun, G. S. Summy, I. Guarneri, S. Wimberger, S. Fishman, and A. Buchleitner, “Decoherence as a probe of coherent quantum dynamics,” *Phys. Rev. E*, vol. 69, p. 027201, Feb 2004. [Online]. Available: <https://link.aps.org/doi/10.1103/PhysRevE.69.027201>
- [17] S. Dadras, A. Gresch, C. Groiseau, S. Wimberger, and G. S. Summy, “Quantum walk in momentum space with a bose-einstein condensate,” *Phys. Rev. Lett.*, vol. 121, p. 070402, Aug 2018. [Online]. Available: <https://link.aps.org/doi/10.1103/PhysRevLett.121.070402>
- [18] C. Groiseau and S. Wimberger, “Spontaneous emission in quantum walks of a kicked bose-einstein condensate,” *Phys. Rev. A*, vol. 99, p. 013610, Jan 2019. [Online]. Available: <https://link.aps.org/doi/10.1103/PhysRevA.99.013610>
- [19] F. M. Izrailev, “Simple models of quantum chaos: Spectrum and eigenfunctions,” *Phys. Rep.*, vol. 196, pp. 299–392, Nov. 1990. [Online]. Available: <https://www.sciencedirect.com/science/article/pii/037015739090067C>
- [20] M. Sadgrove and S. Wimberger, “A pseudoclassical method for the atom-optics kicked rotor: from theory to experiment and back,” in *Advances in Atomic, Molecular, and Optical Physics*. Elsevier, 2011, vol. 60, pp. 315–369.
- [21] G. Summy and S. Wimberger, “Quantum random walk of a Bose-Einstein condensate in momentum space,” *Physical Review A*, vol. 93, no. 2, p. 023638, 2016.

Ringraziamenti

Non sono decisamente bravo con i discorsi, quindi, brevemente, vorrei ringraziare soprattutto il prof. Sandro Wimberger per avermi accettato come laureando in una tesi in Fisica, nonostante sia solo un povero ingegnere. Lo ringrazio anche per il tempo che mi ha dedicato e per la disponibilità e la splendida personalità che ha dimostrato di avere. Ringrazio inoltre il prof. Alberto Bononi per avermi aiutato ad intraprendere questo percorso di studi, risolvendo tutti i problemi burocratici e non che si presentavano. Ringrazio anche il prof. Renato Portugal per avermi fornito un aiuto per una dimostrazione e Francesco Petiziol per la pazienza e i consigli che mi ha dato durante la tesi. Quasi per finire ringrazio gli amici tutti, quelli di fisica, quelli di ingegneria, quelli che si sono persi, quelli di giù, quelli di Parma e quelli sparsi per l'Italia. E per ultimo ma non per questo meno importante, ringrazio tutta la mia famiglia che mi ha supportato in questo viaggio che, comunque, non è ancora finito.